Journal of Constructional Steel Research 143 (2018) 62–71

Contents lists available at ScienceDirect

Journal of Constructional Steel Research

Fire tests on composite steel-concrete beams prestressed with external tendons

Huanting Zhou[a,*], Shaoyuan Li[a], Lu Chen[b], Chao Zhang[c,1]

[a] School of Civil Engineering and Architecture, Wuhan University of Technology, Wuhan 430072, China
[b] China Construction Seventh Engineering Division. Corp. Ltd, Zhengzhou 450004, China
[c] College of Civil Engineering, Tongji University, Shanghai 200092, China

ARTICLE INFO

Article history:
Received 11 August 2017
Received in revised form 5 December 2017
Accepted 6 December 2017
Available online xxxx

Keywords:
Fire resistance
Prestressed structure
Composite steel-concrete beam
Experimental study
Cable strands
Finite element model

ABSTRACT

This paper presents an experimental study on fire resistance of composite steel-concrete beams prestressed with external tendons. A total of four beams were tested under combined fire load and positive moment. Parameters investigated include load level, prestress level and type of cable strands configuration. Results show that the tested beams without fire protection had fire resistance of 20 min to 30 min. The fire resistance of composite steel-concrete beams prestressed with external tendons was highly influenced by the stress in the cable strands. The tested beams with bent-up cable strands had more fire resistance than the tested beams with straight cable strands. Prestress level had little influence on failure temperature of the tested beams, but the slack of cable strands induced failure of the test beams at high temperature. Furthermore, a finite element (FE) model was developed and successfully used to predict the fire behavior of the prestressed composite steel-concrete beams.

1. Introduction

In comparison with the conventional non-prestressed composite steel-concrete beams, prestressed composite beams have several advantages, including elastic behavior under heavier loads, increased ultimate capacity, reduced structural steel weight, more crack resistance (of concrete), and improved fatigue and fracture behavior [1]. Composite beams prestressed with external tendons are mainly used in bridge engineering and mostly used to strengthen existing structures [2], while they have also been used in building structures [3].

To date, there are several studies on the behavior of prestressed composite beams. Saadatmanesh et al. [1,4] analytically and experimentally studied the behavior of prestressed composite steel-concrete beams. Two tendon configurations were considered: straight tendon below the lower flange of the I steel section (for positive moment) and straight tendon below the upper flange (for negative moment). Troitsky et al. [5] analytically and experimentally studied the behavior of simply supported prestressed composite steel-concrete beams. Three tendon configurations were considered: straight (above the lower flange), bent up and short straight (below the lower flange). Ayyub et al. [6] experimentally studied the behavior of prestressed composite steel-concrete beams under positive moments. Various tendon types and configurations were considered. Chen [7] experimentally studied the behavior of prestressed composite steel-concrete beams under negative moments. Lorenc and Kubica [2] experimentally studied the influence of shear connection flexibility on the behavior of prestressed composite steel-concrete beams. However, there is few experimental data on fire behavior of prestressed composite steel-concrete beams. Kang et al. [8] reported fire tests on prestressed composite beams with corrugated webs. Key test variables were the cover thickness of the fire protection material applied to the bottom flange of corrugated webs. The study found that prestressed composite beams with relatively thin fire protection material cover thickness, compared with the non-prestressed slim-floor composite beam, satisfied the required fire performance criteria in the ISO 834 standard.

Previous studies show that prestressed structures are more sensitive to fire than the non-prestressed structures [9–11]. When exposed to fire, the external tendons may become slack due to thermal expansion and, consequently, the prestressed structures with external tendons may fail at a rapid rate. Although the fire behaviors of conventional composite steel-concrete beams have been

* Corresponding author.
E-mail address: zhouht@whut.edu.cn (H. Zhou).
[1] Currently guest scientist at NIST.

https://doi.org/10.1016/j.jcsr.2017.12.008
0143-974X/

well investigated and design methods are developed for composite steel-concrete beams [12], it's still necessary to study the fire behavior of prestressed composite steel-concrete beams because of the significant differences between the behaviors of non-prestressed and prestressed beams. This paper reports an experimental study on the fire behavior of composite steel-concrete beams prestressed with external tendons.

Table 1
Summary of fire test cases.

Beam	Cable configuration	Load ratio	Prestress ratio
PCB-1	Straight	0.35	0.7
PCB-2	Straight	0.35	0.6
PCB-3	Straight	0.22	0.7
PCB-4	Bent up	0.22	0.7

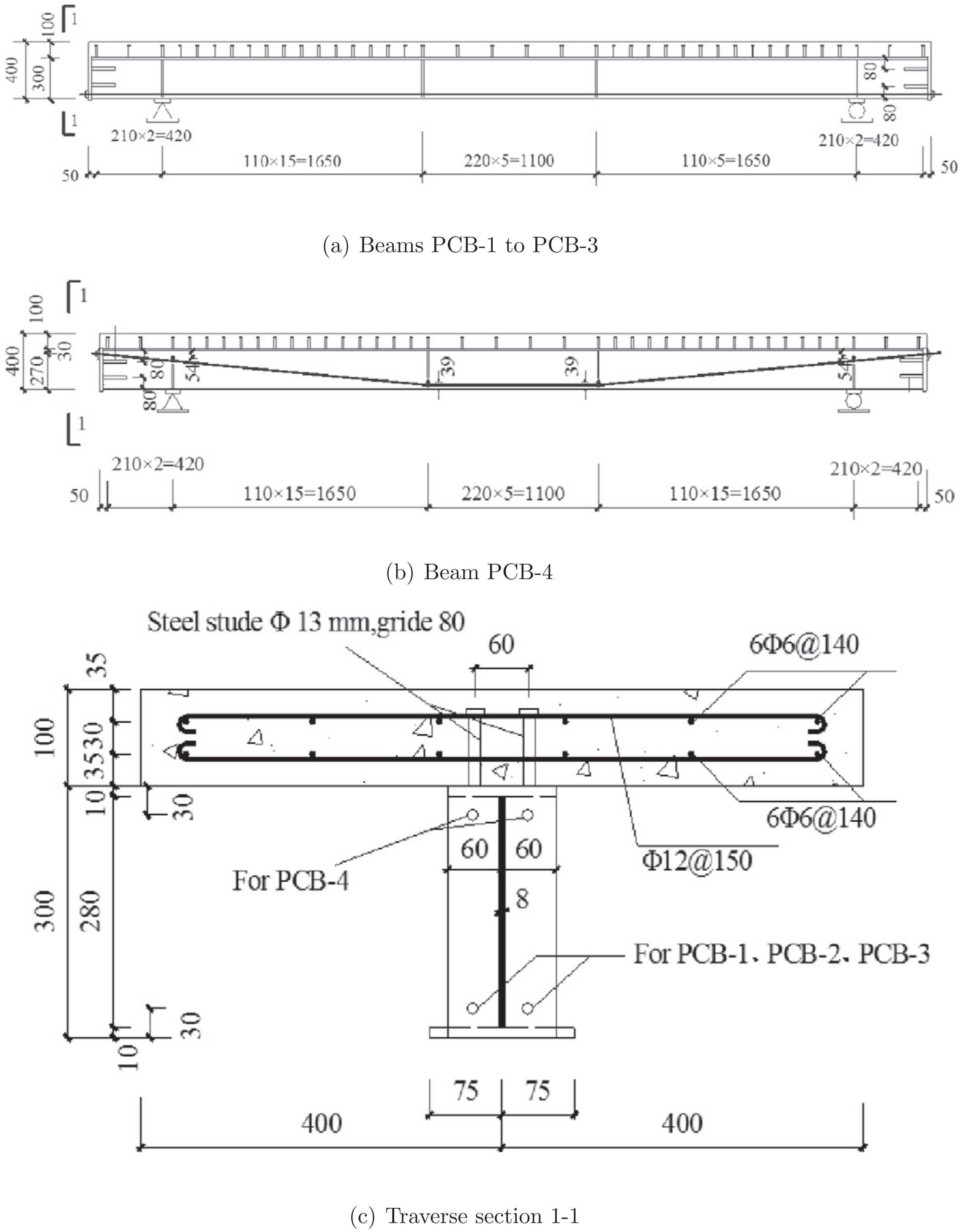

Fig. 1. Details of prestressed composite beams.

Fig. 2. Illustration of fabricated beam PCB-1 to PCB-4 before poring of concrete.

Fig. 3. The utilized furnace and the composite beams placement within the furnace.

2. Experimental description

2.1. Test specimens

Fig. 1 gives details of the test specimens. The prestressed composite beams consisted of a built-up steel section, a reinforced concrete slab and two cable strands. A total of four prestressed composite beams were tested, which were labeled as PCB-1 to PCB-4 and were designed according to the Chinese code for steel structures [13]. Two cable strand configurations were considered: straight (for PCB-1 to PCB-3) and bent up (for PCB-4). Various load ratios (defined as the ratio of the applied force to the ultimate force at ambient temperature) and prestress ratios (defined as the ratio of the applied prestress to the yield strength of the cable strands at ambient temperature) were considered, as summarized in Table 1. The post-tensioning method was used to apply pretension forces. The load ratios were 0.35 for beams PCB-1 and PCB-2, and 0.22 for beams PCB-3 and PCB-4. The prestress ratios were 0.7 for beams PCB-1, PCB-3 and PCB-4, and was 0.6 for beam PCB-2. All beams had the same cross section of 150 mm (bottom flange) × 120 mm (top flange) × 300 mm (height) × 8 mm (web thickness) × 10 mm (flange thickness), same length of 5.3 m and same supporting length of 4.4 m. Bearing stiffeners were welded to the steel beam at the supporting and loading points. The dimensions for stiffeners 1 to 6 (see Fig. 1a–b) were 56 mm (width) × 280 mm (length) × 15 mm (thickness), 120 mm × 320 mm × 20 mm, 56 mm × 190 mm × 15 mm, 56 mm × 220 mm × 15 mm, 120 mm × 320 mm × 20 mm, and 100 mm × 56 mm × 20 mm. Additional endplates were welded at the beam ends to anchor the prestressed cable strands in the beams. The material used for build-up steel section was Q235 steel (nominal yield strength is 235 MPa) and for the prestressed cable strands was a high strength steel with yield strength of 1862 MPa. All beams were designed to achieve full composite action through welding two rows of shear studs with 13 mm diameter to the surface of top flange, as shown in Fig. 2. The concrete slab was 800 mm width and 100 mm thick.

2.2. Test equipment

Fire resistance tests were carried out using a furnace for horizontal building members at the State Key Laboratory at South China Technology University. The furnace can simulate combined loading conditions of temperature, force and restraining boundary conditions to which a building member may be exposed during a fire incident. The test furnace is restrained by a steel frame which is located in the four corners of the chamber. The dimension of the chamber is 3 m (width) × 4 m (depth) × 1.5 m (height). Around the four walls of the chamber, eight natural gas burners were located to provide thermal energy. Additionally, three type-K Chromel-Alumel thermocouples were placed in the chamber to monitor the furnace temperature during a test. The furnace temperature can be programmed to follow any specified fire curves. Fig. 3 shows the furnace with a test specimen.

2.3. Instrumentation

Thermal and mechanical response of the tested beams during fire tests were monitored by thermocouples and displacement transducers. Fig. 4 shows the locations of the thermocouples in measured cross sections. Type-k thermocouples were installed at bottom flange, web, and top flange of the steel section and along the depth of concrete slab. Temperatures of the prestressed cable strands were measured by thermocouples bonded on the surface of the cable strands. Two linear variable displacement transducers (LVDTs) were attached to the top of the concrete slab to measure the mid-span deflection, and two additional LVDTs were placed at both ends of the build-up steel beam to obtain relative axial deformation between the concrete slab and the steel beam. Data from the thermocouples and LVDTs were recorded at 5 s intervals through acquisition system during the fire test.

2.4. Test condition and procedure

Two point loads, each of 98.5 kN (load ratio of 0.35), were applied for PCB-1 and PCB-2 beams. The pretension forces for PCB-1 and PCB-2 were 71.4 kN (prestress ratio of 0.7) and 61.2 kN (prestress ratio of 0.6) respectively. For PCB-3 and PCB-4 beams, two point loads, each of 60/2 kN (load ratio of 0.22), were applied, and the pretension forces for both beams were 71.4 kN.

All beams were three-side exposed to fire. The test beams were placed on the supporters of the furnace (Fig. 3). The fire exposure

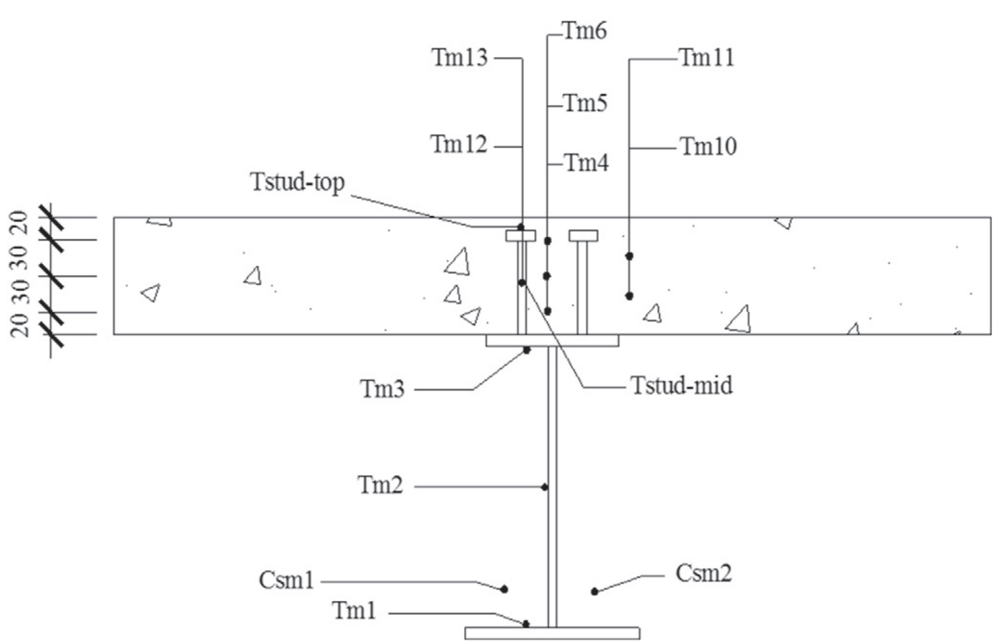

Fig. 4. Location of thermocouples.

length was 4400 mm. The furnace was covered with a specially insulated lid. Prior to fire tests, each beam was preloaded and unloaded twice to minimum the possible gap between the beams and the instrumentation. After that, loads were applied gradually until reaching the target values. The target forces were then maintained for 30 min before heating started. The furnace temperature was designed to follow the ISO834 standard fire curve. The fire test terminated either when the deflection exceeded the stroke of hydraulic actuator or when the working load cannot be sustained by the tested beam.

2.5. Mechanical properties

Mechanical properties of steel, concrete and high-strength steel cable strands were tested in accordance with Chinese codes [13]. Three coupons were cut from steel beams in PCB-1 and PCB-2, and three other coupons were cut from the prestressed cable strands. Concrete cubes were cast from concrete batch mix during fabrication of slab. The 60-day compressive strength for concrete was 34.6 MPa. The yield strength for rebar and steel (of steel beam) were 360 MPa and 315, respectively.

3. Experimental results

3.1. Thermal response

Fig. 5 shows the measured temperatures in the mid-span section of beam PCB-4. Temperature gradient along the beam length was found to be negative. Measured temperatures in the other beams were similar to those in PCB-4. The furnace temperature curve was initially lower than and then close to the ISO834 standard fire curve. For the initial heating period up to 700 s, the web temperature (Tm2) increased faster than the bottom flange temperature (Tm1), because of the thinner thickness of the web (Fig. 5a). After 700 s, the differences between the web and bottom flange temperatures became ignorable. The top flange temperature was constantly lower than both the web and bottom flange temperatures, mainly because of heat conduction from the steel to concrete. As shown in Fig. 5b, the temperatures of cable strands (GJXm3 and GJXm4) rise rapidly. At the final stage of fire exposure, the temperature on the cable strands approached the furnace temperature. The temperature of concrete slab in composite section increased slowly and steadily in comparison with the temperature of steel beam section (Fig. 5c).

3.2. Structural response

3.2.1. Mid-span deflection

Fig. 6 shows the developments of mid-span deflection for test beams PCB-1, PCB-2, PCB-3, and PCB-4. The X-axis values were temperatures of the bottom flange of the steel section. Fig. 7 shows the developments of prestress ratio in cable strands for test beams PCB-1, PCB-2, PCB-3, and PCB-4. Table 2 gives the failure temperature, failure time and maximum deflection for each test. Here, failure temperature is defined as the maximum temperature in the steel beam at failure.

The deflection behavior of beam PCB-1 can be divided into three stages (Fig. 6a). From 20 °C to 230 °C (stage 1), the deflection increased linearly and slowly. At this stage, the decreases of strength and elastic modulus of steel and concrete materials were ignorable, and the increase in deflection was mainly caused by the thermal bowing induced by temperature gradient through the cross section. From 230 °C to 529 °C (stage 2), the deflection increased more quickly. At this stage, the pretension forces in cable strands decreased significantly due to the fire induced thermal strains (Fig. 7a), and also the material properties of steel and concrete reduced considerably. Above 529 °C (stage 3), the deflection increased rapidly, which was caused by the slackness of the cable strands and deterioration of the material properties of steel and concrete. At this stage, the prestress ratios were less than 0.1 (Fig. 7a), which showed that the influence of pretension force in the cable strands on the deflection of the tested beam was important.

Beam PCB-2 showed similar linear deflection behavior with beam PCB-1 in the early stage of heating (stage 1), while the linear behavior of PCB-2 ended at higher temperature (283 °C in Fig. 6b). After

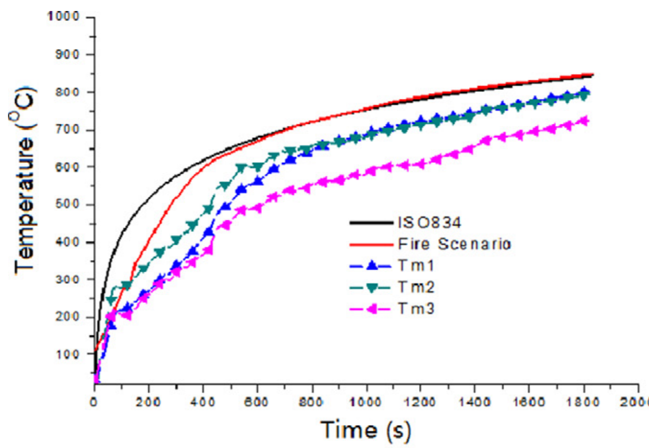

(a) Steel beam

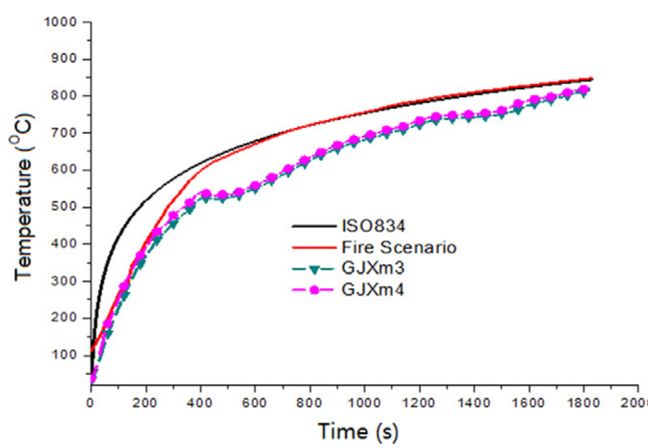

(b) Prestressed cable strands

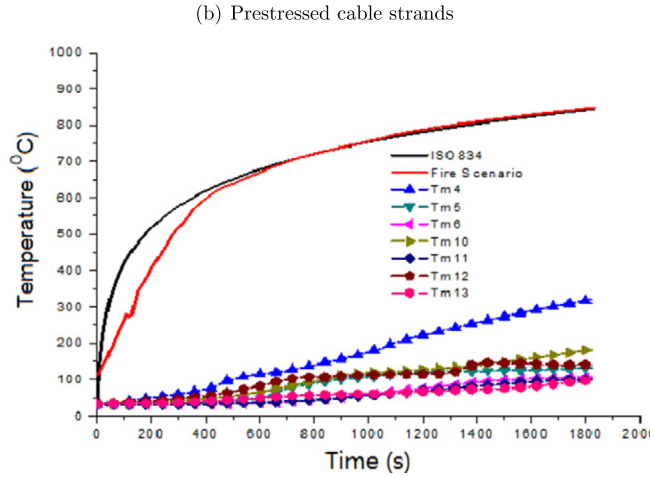

(c) Concrete slab

Fig. 5. Temperature of beam PCB-4.

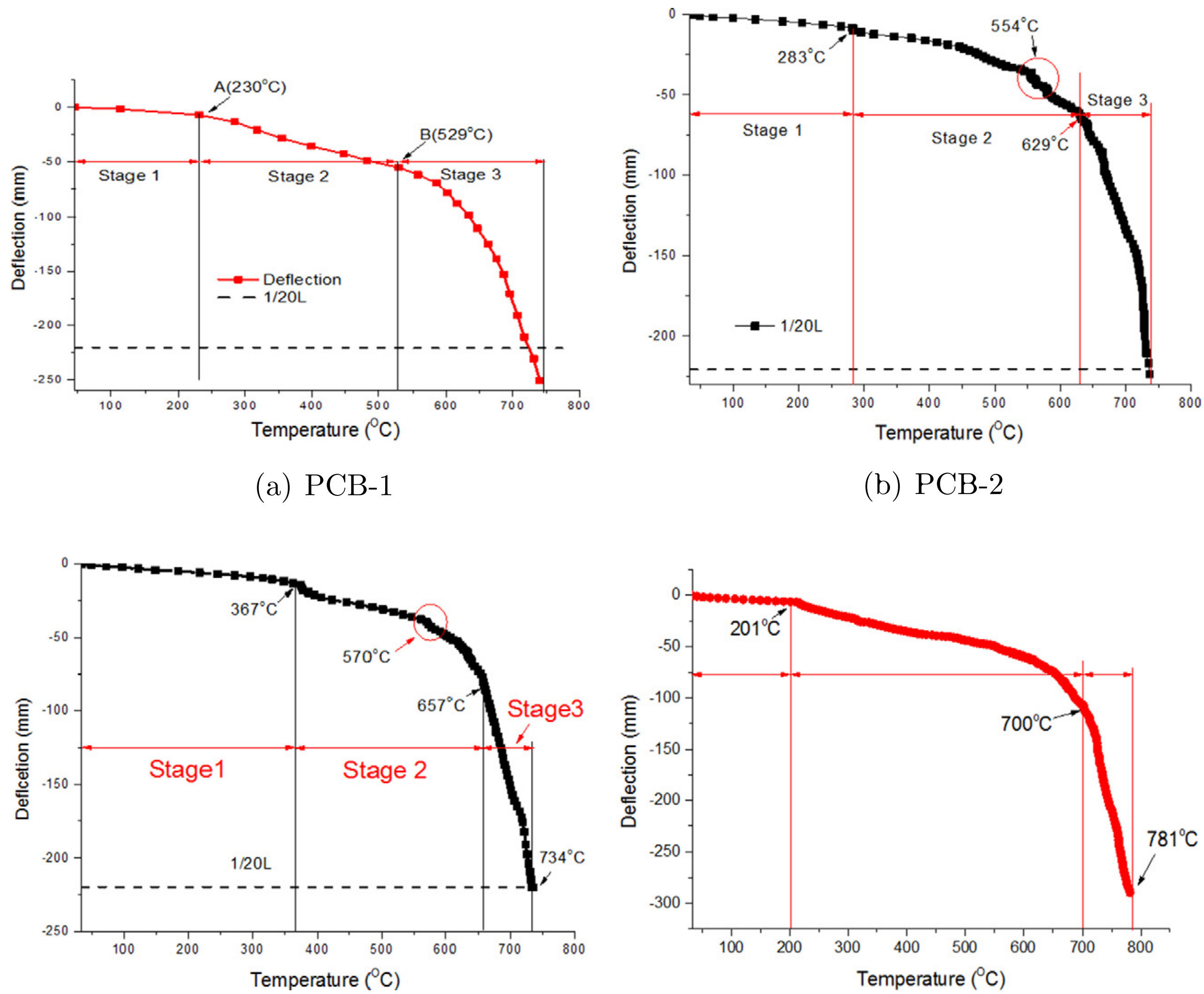

(a) PCB-1
(b) PCB-2
(c) PCB-3
(d) PCB-4

Fig. 6. Temperature-deflection curves.

the early stage, because of the slower degradation of prestress force in the cable strands for PCB-2 (Fig. 7a–b), the deflection of PCB-2 increased slower than that of PCB-1. For the final stage (the diagram was only drawn to 1/20 span due to overlarge deflection) (stage 3), the deflection of PCB-2 increased rapidly, similar to the behavior of PCB-1. Fig. 7b shows that the cable strands became slack at 750 °C, at which the beam PCB-2 reached its failure state.

Beam PCB-3 showed similar linear deflection behavior to beam PCB-1 in the early heating stage (stage 1). After the early stage, deflection of PCB-3 increased slower than that of PCB-1, because of the lower load ratio for PCB-3. For the final stage (the diagram was only drawn to 1/20 span due to overlarge deflection), the deflection of PCB-3 increased rapidly. Fig. 7c shows that the cable strands became slack after 657 °C. Drop of the prestress in cable strands had important negative effect on the transverse stiffness of the tested beam. As shown in Figs. 6c and 7c, the prestress ratio curve had a slight fluctuation at 570 °C and the deflection curve also had a local peak value at this temperature, which showed that the prestress in cable strands had important effect on the transversal stiffness of prestressed composite beam at high temperature. When the cable strands became slack, the deflection of the composite beam increased rapidly.

Beam PCB-4 showed similar linear deflection behavior to PCB-3 at the early heating stage (stage 2). After the early stage, prestress in cable strands of PCB-4 decreased considerably at 201 °C (Fig. 7c). At the final stage (stage 3), the deflection of beam PCB-4 increased rapidly. Fig. 6c–d shows that the deflection of PCB-4 developed slower than that of PCB-3 in stage 3, because of the different configuration of cable strands in the two beams. The shape of bent-up cable strands in PCB-4 was consistent with the moment diagram of the beam subjected to concentrated loads, which made PCB-4 to be more fire resistant than PCB-3 (with straight cable strands).

3.2.2. Axial slip

The measured axial slip at the ends of PCB-1 to PCB-4 versus the temperature of bottom flange is plotted in Fig. 8. The slip between beam and concrete slab was negligible between 20 °C and 300 °C. This is because within this temperature, shear strength of the shear studs on the top flange of steel beams has small change (because strength and elasticity of concrete and steel are nearly not changed). When temperature was above 300 °C, the slip increased with temperature. This is caused by the drop of the shear stiffness of the shear studs (because of temperature rise). However, the magnitudes of slip of the tested beams were negligible (less than 0.1 mm in all beams). The results indicated that the composite beams had full shear connection at high temperature.

Table 2
Summary of fire test results.

Beam	Failure temperature (°C)	Maximum deflection (mm)	Failure time (min)
PCB-1	741	252.0	21
PCB-2	753	272.8	23
PCB-3	779	304.9	29
PCB-4	806	298.8	30

3.2.3. Failure modes

Fig. 9 shows the failure modes of beams PCB-1 to PCB-4. All beams failed by losing flexural strength at high temperature. The ratios of width to thickness for flange and web plates were 5.6 and 35, respectively. According to the BS5950 [14], the steel section was a plastic section. The plates of the built-up steel beam did not have local buckling at high temperature, which was consistent with the prediction for plastic section.

As shown in Fig. 9, cracks were found on the side surfaces of the concrete slabs, which indicated that the concrete slabs experienced high tension stress at elevated temperature. At ambient temperature, under positive moment the concrete slab was in compression and the neutral axis of the composite section was in the steel section. When exposed to fire, the neutral axis of the composite section moved upward because of the degradation of material properties and the slackness of the cable strands at elevated temperature. When the test beams approaching failure at elevated temperature, the neutral axes were in the concrete section. Therefore, the concrete sections below the neutral axes were under tension and would have cracks due to lower tension strength at high temperature.

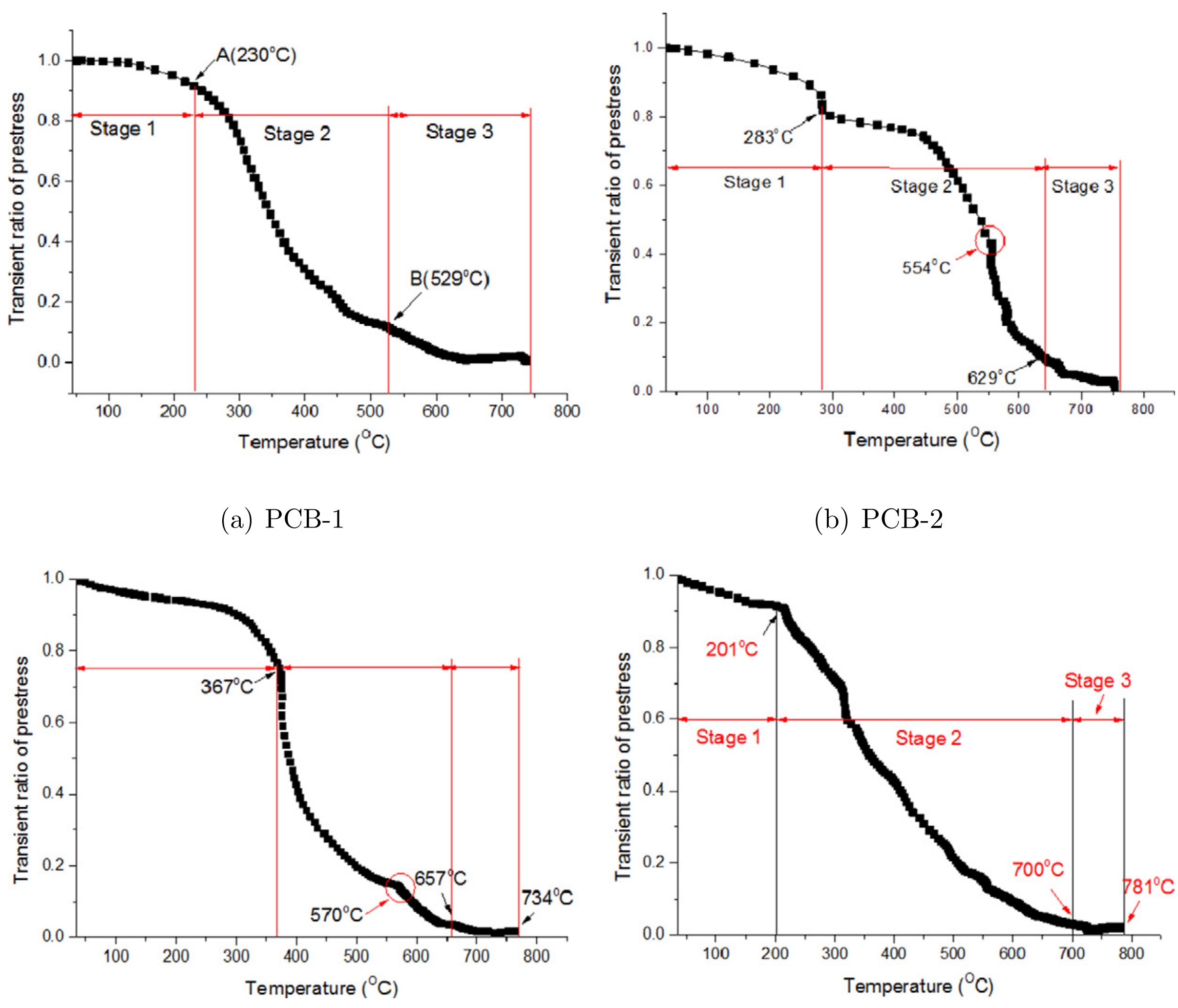

(a) PCB-1 (b) PCB-2

(c) PCB-3 (d) PCB-4

Fig. 7. Temperature-prestress ratio (or ratio of prestress) curves.

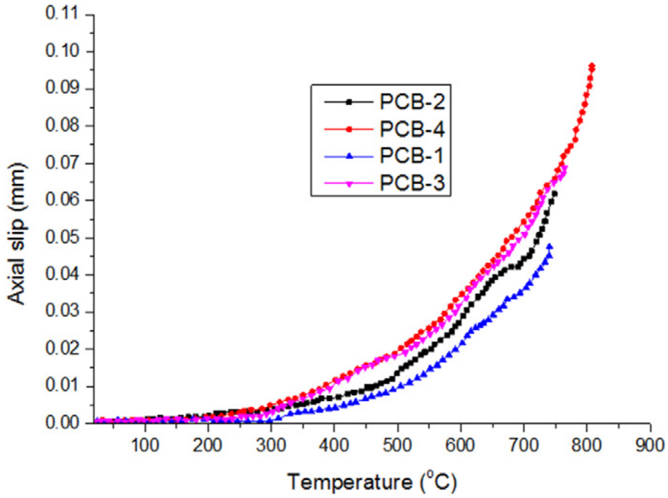

Fig. 8. Comparison of axis slip for beams PCB-1 to PCB-4.

4. Numerical study

To better understand the fire behaviors of prestressed composite beams, numerical simulations using the finite element (FE) software ABAQUS [15] were conducted to model the fire tests described above. Fig. 10a shows the FE model. In the FE model, the concrete slab was meshed using solid element (DC3D8 for heat transfer analysis and C3D8 for structural analysis), the steel beam was meshed using shell element (DS4 for heat transfer analysis and S4 for structural analysis) and the rebars and tendons were meshed using link element. In the FE thermal model, the top surface of the upper flange of the steel beam was assumed to be perfected tied with the bottom surface of the concrete slab that there had no temperature gradient at the steel-concrete interface. The steel beam was three-side exposed to fire, the bottom surface of the concrete slab was exposed to fire and the top surface of the slab was exposed to ambient temperature. According to the Eurocode [16], the convective heat transfer coefficients were taken as 25 W/(m°C) and 4 W/(m°C) for fire exposed and unexposed surfaces, respectively. The emissivities of steel and concrete were taken as 0.7. The temperature-dependent thermal properties for steel and concrete given in the Eurocode [17,18] were used in the FE thermal model. In the FE structural model, connection element CONN3D2 was used to model the slip effect of the stubs. The high temperature mechanical properties for concrete and structural steel were taken from the Eurocode [17,18]. Strain-hardening effect for structural steel was considered. The material properties for tendons were taken from Ref. [19] and the material properties for the steel stubs were taken from Ref. [20]. As shown in Figs. 10c and 11, the FE model adequately predicted the fire tests on the prestressed composite beams.

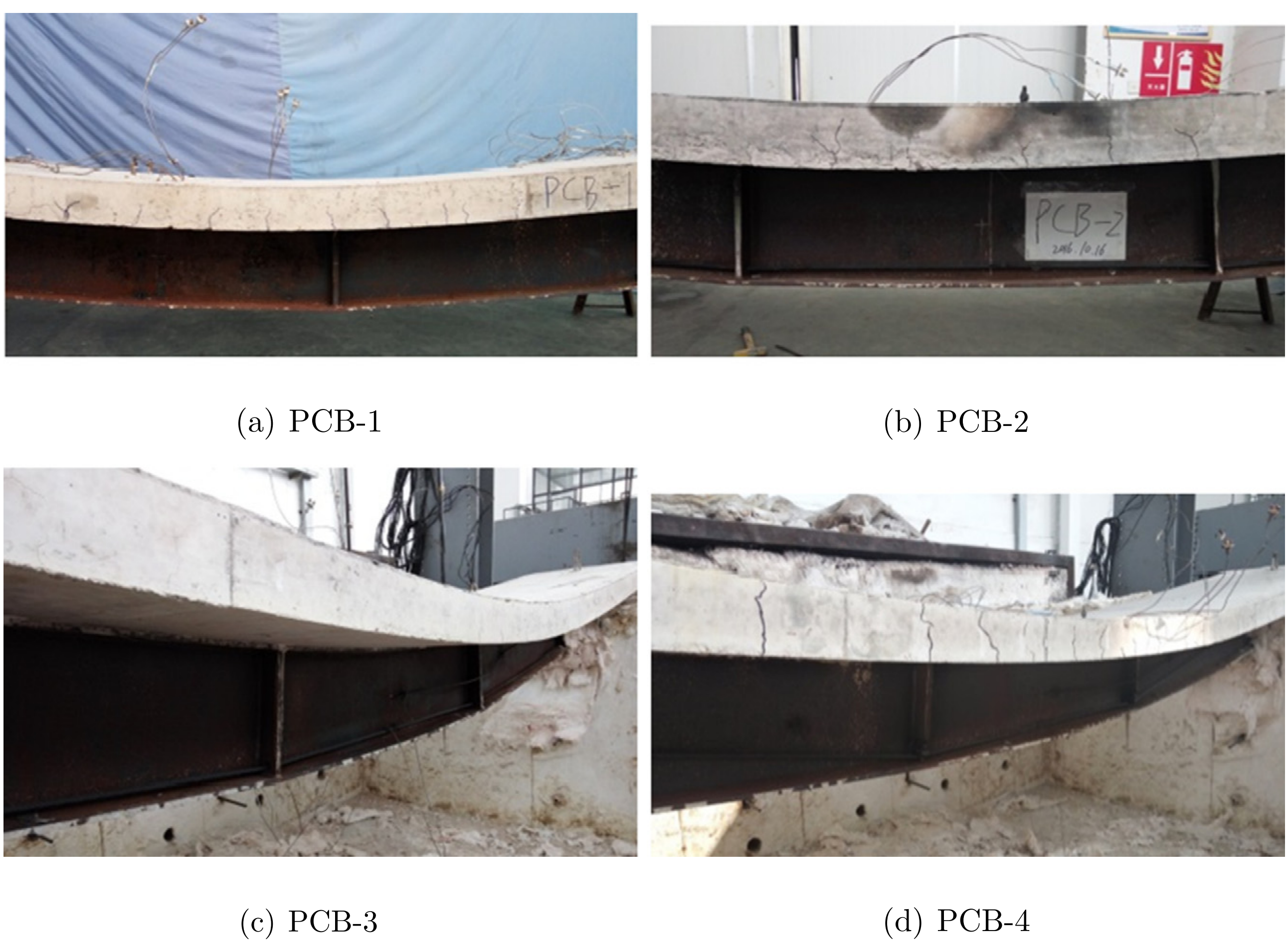

(a) PCB-1 (b) PCB-2

(c) PCB-3 (d) PCB-4

Fig. 9. Failure modes of beam PCB-1 to PCB-4.

5. Conclusion

This paper presents the experimental study of prestressed composite beams subjected to fire and positive moment. The parameters investigated include load ratio, prestress ratio, and the configuration of prestressed cable strands. Based on the test results, the following conclusion can be drawn:

- The investigated prestressed composite beams without fire protection have fire resistance of 20 min to 30 min. The stress in cable strands at elevated temperature has important influence on the beam behavior.
- The tested composite beams prestressed by bent-up cable strands have higher fire resistance than the tested beams prestressed by straight cable strands.
- Load ratio has negative effect on the failure temperature of prestressed composite beams, the greater the load ratio, the lower the failure temperature. The effect of initial prestress in the cable strands on failure temperature is not significant in the tested beams, while the slackness of the cable strands causes failure of the beams at elevated temperature.
- The numerical model developed in this paper adequately predicts the fire behaviors of the prestressed composite beams, which can be used in further parametric studies.

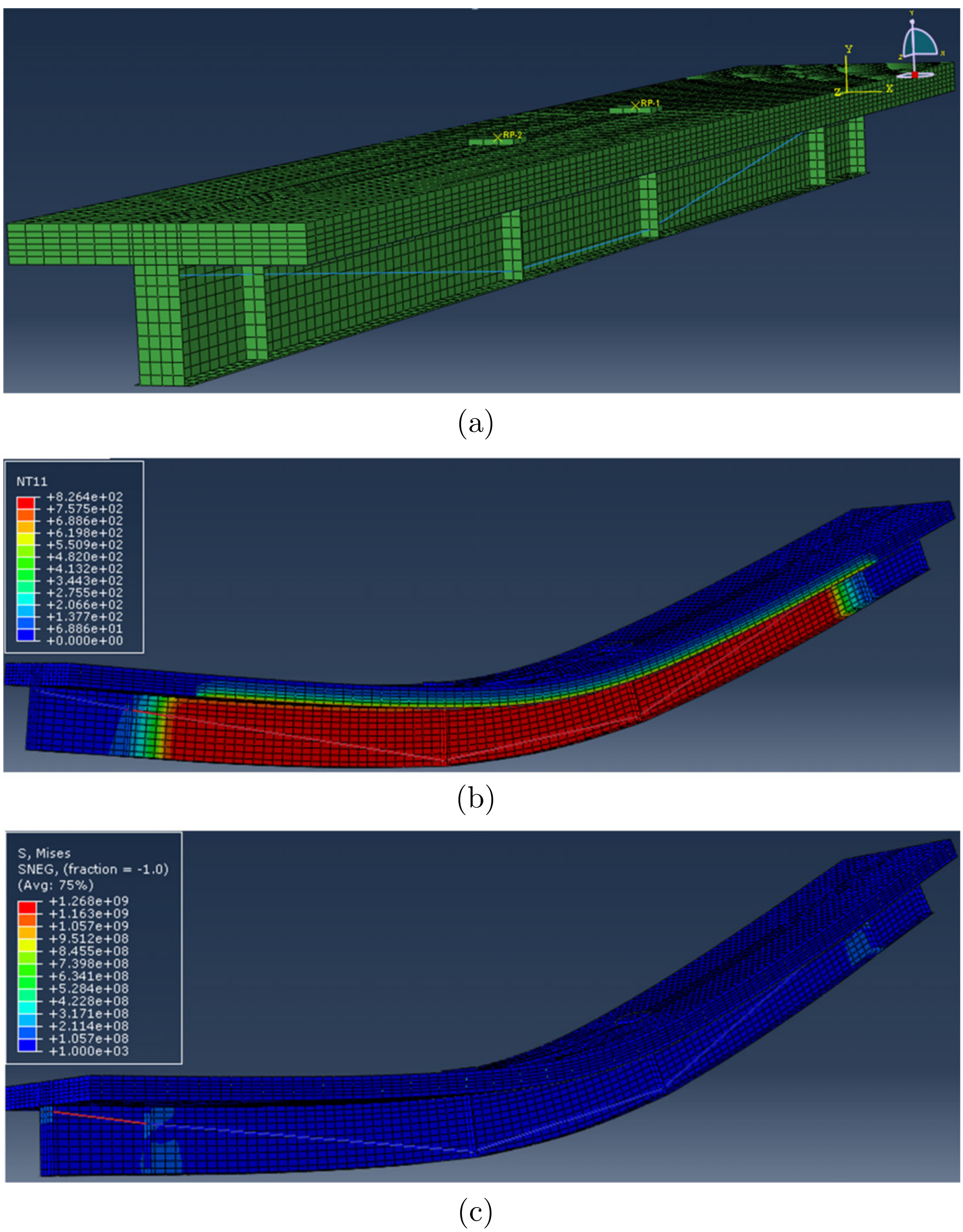

Fig. 10. FE model and numerical results. (a) FE model for PCB-4; (b) Distribution of temperature in PCB-4 at heating time of 30 min; (c) Distribution of stress in PCB-4 at failure.

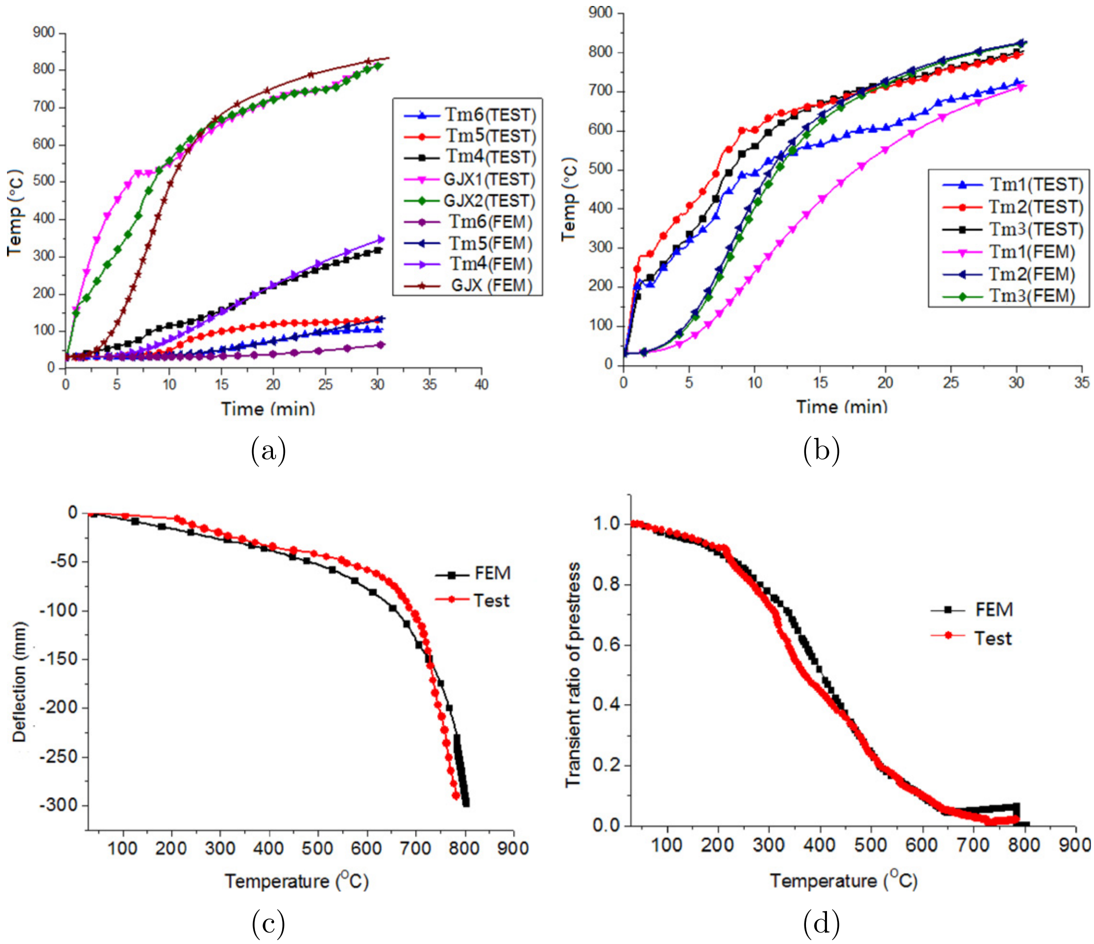

Fig. 11. Comparison between numerical results and test data. (a) Temperatures in concrete slab; (b) Temperatures in steel beam; (c) Deflection for PCB-4; (d) Prestress.

Acknowledgments

The work reported in this paper is partially supported by the National Science Foundation of China through contract nos. 51278394, 51508399. The support is gratefully acknowledged.

References

[1] H. Saadatmanesh, P. Albrecht, B.M. Ayyub, Experimental study of prestressed composite beams, J. Struct. Eng. 115 (1989) 2348–2363.
[2] W. Lorenc, E. Kubica, Behavior of composite beams prestressed with external tendons: experimental study, J. Constr. Steel Res. 62 (2006) 1353–1366.
[3] S.M. Chen, P. Gu, Load carrying capacity of composite beams prestressed with external tendons under positive moment, J. Constr. Steel Res. 61 (2005) 515–530.
[4] H. Saadatmanesh, P. Albrecht, B.M. Ayyub, Analytical study of prestressed composite beams, J. Struct. Eng. 115 (1989) 2364–2381.
[5] M.S. Troitsky, Z.A. Zielinski, A. Nouraeyan, Pre-tensioned and posttensioned composite girders, J. Struct. Eng. 115 (1989) 3142–3153.
[6] B.M. Ayyub, Y.G. Sohn, H. Saadatmanesh, Prestressed composite girders under positive moment, J. Struct. Eng. 116 (1990) 1931–2951.
[7] S.M. Chen, Experimental study of prestressed steel-concrete composite beams with external tendons for negative moments, J. Constr. Steel Res. 61 (2005) 1613–1630.
[8] H. Kang, D.H. Lee, J.H. Hwang, J.Y. Oh, K.S. Kim, H.Y. Kim, Structural performance of prestressed composite members with corrugated webs exposed to fire, Fire Technol. 52 (2016) 1957–1981.
[9] L.A. Ashton, H.L. Malhotra, The fire resistance of prestressed concrete beams, Fire Res. Notes (1953) 65.
[10] A.H. Griffin, M. Beavis, Fire Resistance of Prestressed Concrete, University of Canterbury. 1992.
[11] C. Maluk, G.P. Terrasi, L. Bisby, A. Stutz, E. Hugi, Fire resistance tests on thin CFRP prestressed concrete slabs, Construct. Build Mater. 30 (2015) 558–571.
[12] J. Kruppa, B. Zhao, Fire resistance of composite beams to Eurocode 4 Part 1.2, J. Constr. Steel Res. 33 (1995) 51–69.
[13] GB50017-2003. Code for Design of Steel Structures, China Planning Press, Beijing, 2003.(in Chinese).
[14] BS5950, Structural Use of Steelwork in Building - Part 1: Code of Practice for Design - Rolled and Welded Sections, 2001.
[15] ABAQUS.ABAQUS/Standard Version 6.12 Users Manuals: Volume IIII, Hibbitt,Karlsson, and Sorenson Inc. Pawtucket.
[16] Eurocode 1: Actions on Structures - Part 1-2: General Actions - Actions on Structures Exposed to Fire, British Standards. 2002.
[17] Eurocode 3: Design of Steel Structures - Part 1–2: General Rules - Structural Fire Design, British Standards. 2005.
[18] Eurocode 4: Design of Composite Steel and Concrete Structures - Part 1–2: General Rules - Structural Fire Design, British Standards. 2005.
[19] H.T. Zhou, G.Q. Li, S.C. Jiang, Experimental studies on the properties of steel strand at elevated temperatures, J. Sichuan Univ. 5 (2008) 106–110. in Chinese.
[20] L.Z. Chen, G.Q. Li, S.C. Jiang, Experimental studies on behavior of headed stud shear connectors at elevated temperatures, J. Tongji Univ. 41 (2013) 1151–1157. In Chinese.